

# Targeting of astrocytic glucose metabolism by beta-hydroxybutyrate

Rocío Valdebenito<sup>1</sup>, Iván Ruminot<sup>2</sup>, Pamela Garrido-Gerter<sup>1,3</sup>, Ignacio Fernández-Moncada<sup>1,3</sup>, Linda Forero-Quintero<sup>2</sup>, Karin Alegría<sup>1</sup>, Holger M Becker<sup>2</sup>, Joachim W Deitmer<sup>2</sup> and L Felipe Barros<sup>1</sup>



## Abstract

The effectiveness of ketogenic diets and intermittent fasting against neurological disorders has brought interest to the effects of ketone bodies on brain cells. These compounds are known to modify the metabolism of neurons, but little is known about their effect on astrocytes, cells that control the supply of glucose to neurons and also modulate neuronal excitability through the glycolytic production of lactate. Here we have used genetically-encoded Förster Resonance Energy Transfer nanosensors for glucose, pyruvate and ATP to characterize astrocytic energy metabolism at cellular resolution. Our results show that the ketone body beta-hydroxybutyrate strongly inhibited astrocytic glucose consumption in mouse astrocytes in mixed cultures, in organotypic hippocampal slices and in acute hippocampal slices prepared from ketotic mice, while blunting the stimulation of glycolysis by physiological and pathophysiological stimuli. The inhibition of glycolysis was paralleled by an increased ability of astrocytic mitochondria to metabolize pyruvate. These results support the emerging notion that astrocytes contribute to the neuroprotective effect of ketone bodies.

## Keywords

ATeam, FLIII2Pglu700 $\mu\Delta$ 6, Förster Resonance Energy Transfer microscopy, ketone bodies, pyronic

Received 9 May 2015; Revised 10 July 2015; Accepted 14 July 2015

## Introduction

There is abundant evidence that ketone bodies are neuroprotective. For example, in GLUT1 deficiency, a pediatric condition characterized by impaired glucose delivery through the blood-brain barrier,<sup>1</sup> the treatment of choice is the ketogenic diet.<sup>2,3</sup> Ketone bodies, the ketogenic diet and intermittent fasting have also been shown to be neuroprotective in cell models, animal models and clinical cases of epilepsy, Alzheimer's, Parkinson's and Huntington's disease, neurodegenerative conditions characterized by early local deficits in brain glucose consumption.<sup>4</sup> Underscoring the role of glucose metabolism in neurodegeneration, it was recently reported that Alzheimer's disease is exacerbated by GLUT1 deficiency.<sup>5</sup>

The ketogenic diet and prolonged fasting induce the production of ketone bodies by the liver, mostly beta-hydroxybutyrate (BHB) and acetoacetate, which reach millimolar levels in blood and are oxidized in peripheral

tissues for the production of metabolic energy. Under normal circumstances the brain is almost exclusively fueled by glucose, but if ketone bodies are available, they are efficiently utilized and a reduction of brain tissue glucose consumption is observed.<sup>6,7</sup> The neuroprotective effect of ketone bodies has been linked to changes in glucose metabolism.<sup>8,9</sup> While both neurons and astrocytes can efficiently oxidize ketone bodies,<sup>10</sup> their respective roles on the change in tissue glucose consumption provoked by ketone bodies is not well defined. Before reaching neurons most glucose passes through astrocytes<sup>11</sup> where a fraction is converted to

<sup>1</sup>Centro de Estudios Científicos, Valdivia, Chile

<sup>2</sup>General Zoology/University of Kaiserslautern, Kaiserslautern, Germany

<sup>3</sup>Universidad Austral de Chile, Valdivia, Chile

## Corresponding author:

L Felipe Barros, Centro de Estudios Científicos (CECs), Arturo Prat 514, Valdivia, Chile.

Email: fbarros@cecs.cl

lactate. Lactate may sustain neuronal firing and synaptic activity over short periods,<sup>12,13</sup> but glucose is an absolute requirement for long-term neuronal function, antioxidant and inhibition of apoptosis.<sup>14–16</sup>

The question therefore arises as to whether ketone bodies may modulate the consumption of glucose by astrocytes, affecting the delivery of glucose and lactate to neurons. In the present study we have used Förster Resonance Energy Transfer (FRET) sensors for metabolites to investigate possible effects of chronic exposure to the ketone body BHB on the handling of glucose by astrocytes. Our results *in vitro* and *in vivo* show a strong inhibitory effect on astrocytic glucose usage, pointing to astrocytic metabolism as a possible target for neuroprotection.

## Materials and methods

Standard reagents and inhibitors were acquired from Sigma or Merck. Plasmids encoding the FRET sensors FLII12Pglu700 $\mu\Delta$ 6,<sup>17</sup> ATeam 1.03<sup>18</sup> and Pyronic<sup>19</sup> are available from Addgene ([www.addgene.org](http://www.addgene.org)). Viral vectors Ad FLII12Pglu700 $\mu\Delta$ 6, Ad ATeam and Ad Pyronic (all serotype 5) were custom made by Vector Biolabs. The adeno-associated virus (AAV9) expressing FLII12Pglu700 $\mu\Delta$ 6 under the control of the short gfaABC1D promoter was generated at the École Polytechnique Fédérale de Lausanne, Switzerland. Design, production and titration of the AAV9 vector for transgene expression in astrocytes have been described previously.<sup>20</sup> Magnesium Green acetoxymethyl ester (AM) and SNARF-5F 5-(and-6)-carboxylic acid AM were obtained from Molecular Probes.

## Animals, cultures, stereotaxis and brain slices

Procedures involving animals were carried out according to the Guide for the Care and Use of Laboratory Animals, National Research Council, USA. Procedures were approved by the Centro de Estudios Científicos Animal Care and Use Committee or by the Landesuntersuchungsamt Rheinland-Pfalz, Koblenz (23 177–07). The reports of the procedures comply with the ARRIVE guidelines. Mixed neuronal glial primary cultures (days 8–16) were prepared from mixed F1 1- to 3-day-old mice (C57BL/6J x CBA/J), as described previously.<sup>21</sup> To estimate astrocytic glucose in acute hippocampal slices, 2-month-old female mice (C57BL/6J x CBA/J) were anesthetized with an intraperitoneally injected mixture of ketamine (100 mg per kg bodyweight) and xylazine (10 mg per kg bodyweight). The head was fixed in a stereotactic apparatus and the eyes were kept wet with an ointment (vitamin A eye cream; Bausch & Lomb, Switzerland). A 1.4-mm diameter craniotomy was drilled using a dental drill and

1  $\mu$ L of AAV9-GFAP-FLII12Pglu700 $\mu\Delta$ 6 ( $2.21 \times 10^{14}$  vg/ml) was injected into the hippocampus. The open skin was treated with Lidocaine (4%) and sutured. After surgery the animals were kept warm, monitored until recovery from anesthesia and returned to their cages. The animals were maintained on a 12-h day/night cycle at constant room temperature with free access to water and standard mouse fodder in the animal facility of CECs. The concentration of ketone bodies in urine samples was determined with Ketone Body Assay Kit (EnzyChrom TM). After 6 weeks, animals were killed by cervical dislocation and 200- $\mu$ m-thick coronal hippocampal slices were prepared as described previously.<sup>22</sup> Organotypic hippocampal slice cultures were prepared according to literature<sup>23</sup> with some modifications. In brief, hippocampal slices (400  $\mu$ m) were cut with a McIlwain tissue chopper (Mickle Laboratory Engineering Company, United Kingdom) from 5- to 7-day-old C57BL/6 mice under sterile conditions. Slices were maintained on biopore membranes (Millicell standing inserts, Merck Millipore, Germany) in an interface between humidified normal atmosphere (5% CO<sub>2</sub>, 36.5°C) and culture medium, which consisted of 50% Minimal Essential Medium, 25% Hank's balanced salt solution, 25% horse serum and 2 mM L-glutamine and 5 mM D-glucose at pH 7.4 in an incubator (Mettmert, Germany). The culture medium (1 ml) was renewed every 3 days. After 7 days of culture, the slices were transduced by overnight incubation with  $5 \times 10^6$  PFU of Ad FLII12Pglu700 $\mu\Delta$ 6 and imaged after another 4–8 days. To expose cultured cells and slices to ketone bodies, the culture medium was renewed with fresh culture medium containing 2 mM BHB. Fresh medium without BHB was used as control condition. After 3 days of exposure, cells and slices were transferred to a microscope rig and imaged as described below.

## Fluorescence imaging

Detailed protocols for the use of the fluorescent sensors for glucose, lactate and pyruvate are available.<sup>24–26</sup> Cultured cells and acute slices were imaged with an upright Olympus FV1000 confocal microscope and a 440-nm solid-state laser. Alternatively, cells were imaged with Olympus IX70 or BX51 microscopes equipped with Cairn Research monochromators and Optosplits and either a Hamamatsu Orca or Rollera camera. Cells were superfused at room temperature with a 95% air/5% CO<sub>2</sub>-gassed solution of the following composition (mM): 112 NaCl, 3 KCl, 1.25 CaCl<sub>2</sub>, 1.25 MgCl<sub>2</sub>, 2 glucose, 1 Na-lactate, 10 HEPES and 24 NaHCO<sub>3</sub>, pH 7.4 and tissue slices with a 95% O<sub>2</sub>/5% CO<sub>2</sub>-gassed solution of the following composition (mM): 126 NaCl, 3 KCl, 1.25 NaH<sub>2</sub>PO<sub>4</sub>, 1.25 CaCl<sub>2</sub>,

1.25 MgCl<sub>2</sub>, 10 glucose and 26 NaHCO<sub>3</sub>, at pH 7.4. The intact biopore membrane carrying organotypic hippocampal slices was inserted into the recording chamber of an upright microscope (BX50WI, Olympus) equipped with a monochromator (Polychrome IV, Till Photonics), Optosplit (Cairn Research, UK) and a cooled CCD camera (Till Photonics). The slices were superfused continuously with a CO<sub>2</sub>/HCO<sub>3</sub><sup>-</sup> buffered saline containing (in mM): 136 NaCl, 3 KCl, 2 CaCl<sub>2</sub>, 1 MgCl<sub>2</sub>, 24 NaHCO<sub>3</sub>, 1.25 NaH<sub>2</sub>PO<sub>4</sub>; 2 glucose, 1 lactate, pH 7.4 at room temperature (22–24°C). To measure the permeability mediated by monocarboxylate transporters (MCTs), mixed cultures were loaded with 18 μM SNARF-5F 5- (and -6)-carboxylic acid AM for 15 min at 25°C and imaged with an LSM 700 Zeiss confocal microscope under continued superfusion with a buffer containing (in mM): 140 NaCl, 5 KCl, 2 CaCl<sub>2</sub>, 1 MgCl<sub>2</sub>, 0.5 NaH<sub>2</sub>PO<sub>4</sub>, 10 glucose, 10 HEPES, pH 7.4 at room temperature (22–24°C).

Data are presented as means ± SEM, except during exposure to experimental treatments where SEM are omitted for clarity. Metabolic fluxes are expressed as change in amount of substrate per liter of distribution volume per unit time (μM/s). Fluxes may be translated into more traditional units used for isotopic *in vitro* measurements by taking into account the astrocytic water distribution space (e.g. 6.4 μL/mg of protein<sup>27</sup>). Comparison with data obtained in intact brain tissue, e.g. FDG-PET, may be achieved by considering the distribution space of glucose in brain tissue (0.77 mL/gram of tissue<sup>28</sup>). For example, the rate of glucose consumption reported below in protoplasmic astrocytes (7 μM/s; see below) translates into 0.32 μmol/min per gram. As a reference,

FDG-PET glucose consumption by mouse brain tissue has been measured at 0.61 μmol/min per gram.<sup>29</sup> Differences between experimental groups were assessed with the Student's t-test. *p* values < 0.05 were considered significant and are indicated with an asterisk (\*).

## Results

This work investigated the possible impact of a chronic exposure to ketone bodies on astrocytic energy metabolism. Glucose metabolism was characterized using FLII12Pglu700μΔ6,<sup>17</sup> a genetically-encoded FRET nanosensor for glucose that is insensitive to glucose-6-phosphate.<sup>30</sup> The method for the use of this sensor to quantify glucose consumption is available elsewhere.<sup>21,25</sup> In short, the glucose sensor is expressed in cells (Figure 1a) and glucose consumption is measured by FRET microscopy as the rate of cytosolic glucose depletion after addition of cytochalasin B (Figure 1b), a non-competitive blocker of glucose uptake through GLUT1.<sup>31</sup> Chronic exposure of cultured astrocytes to 2 mM BHB, a concentration similar to that observed in plasma during a ketogenic diet, resulted in an 80% decrease of the rate of glucose consumption (Figure 1c).

The consumption of glucose and production of lactate by astrocytes is acutely modulated by extracellular K<sup>+</sup>,<sup>32–34</sup> the level of which is proportional to the intensity of excitatory synaptic activity and axonal firing.<sup>35</sup> The activation of glycolysis by high [K<sup>+</sup>] in astrocytes is evidenced as a decrease in cytosolic glucose proportional to the degree of metabolic stimulation. As shown in Figure 2(a), after 3 days of exposure to BHB, astrocytes became less sensitive to high K<sup>+</sup>

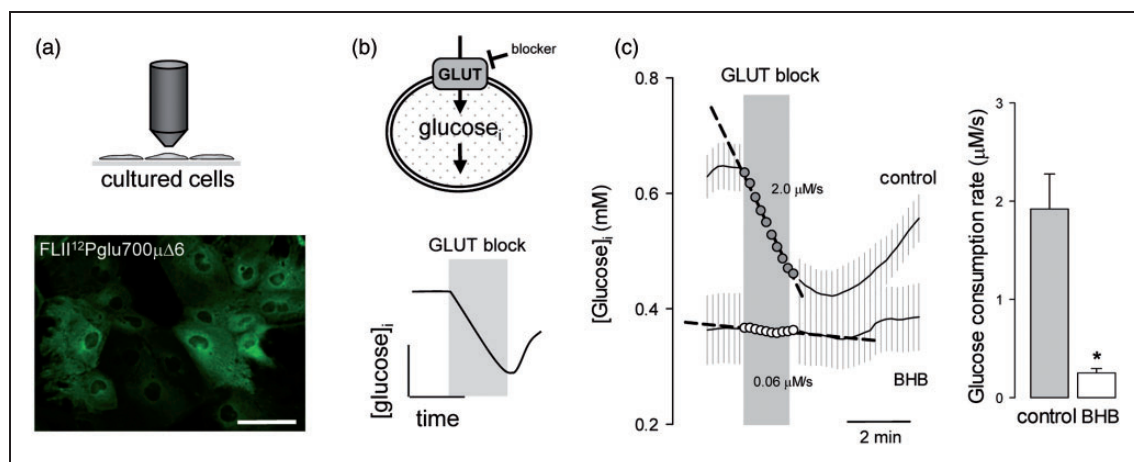


**Figure 1.** Chronic BHB exposure inhibits glucose consumption by cultured astrocytes. (a) Expression of the glucose sensor FLII<sup>12</sup>Pglu700μΔ6 in astrocytes of mixed cortical cultures. Bar = 50 μm. (b) Rationale of the method to measure the rate of glucose consumption by monitoring cytosolic glucose in the presence of the GLUT blocker cytochalasin B (20 μM). (c) Measurement of glucose consumption rates of astrocytes exposed for 3 days to control conditions (gray symbols) or to 2 mM BHB (open symbols). Bars represent the average rates obtained in three separate experiments (20–30 cells per experiment).

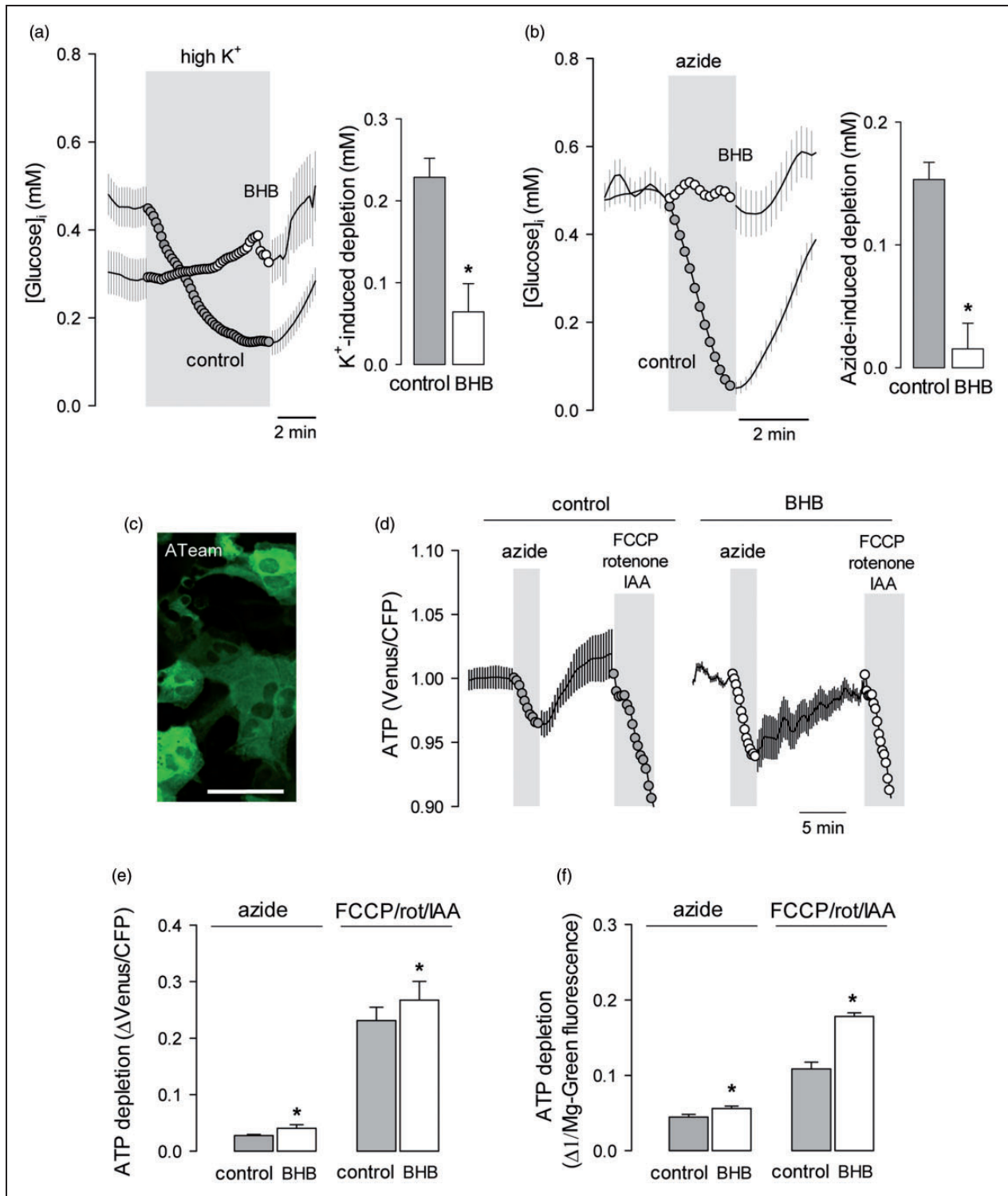


**Figure 2.** Chronic BHB exposure inhibits the stimulation of astrocytic glycolysis by  $K^+$  and OXPPOS inhibition. Effect of raising extracellular  $K^+$  from 3 to 12 mM (a) or inhibiting OXPPOS with 5 mM azide (b) on astrocytic glucose in control cultures (gray symbols) or in cultures exposed for 3 days to 2 mM BHB (open symbols). Bars represent the average extent of glucose depletion recorded after 5 min stimulation in three separate experiments (20–30 cells per experiment). (c) Expression of the FRET ATP sensor ATeam in astrocytes of mixed cortical cultures. Bar = 50  $\mu$ m. (d) Effect of 5 mM azide or a cocktail composed of 2  $\mu$ M FCCP, 2  $\mu$ M rotenone and 500  $\mu$ M iodoacetic acid (IAA) on astrocytic ATP in control cultures (gray symbols) or in cultures exposed for 3 days to 2 mM BHB (open symbols). Data are normalized relative to the beginning of the experiments. (e) Average ATP depletion after 3-min exposure measured with ATeam in three separate experiments similar to those shown in (d) (6–8 cells per experiment). (f) Average ATP depletion after 3-min exposure, measured with the dye Magnesium Green in three separate experiments analogous to those shown in (d) (20–30 cells per experiment).

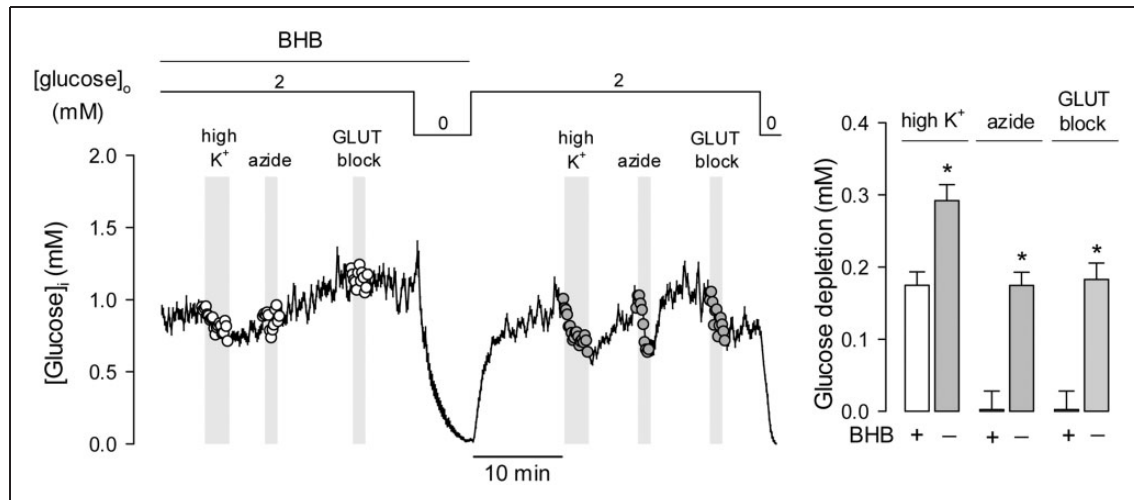


**Figure 3.** The effects of chronic BHB exposure on astrocytic glycolysis are reversible. Cultures were pre-incubated with 2 mM BHB for 3 days and then sequentially exposed to 12 mM  $K^+$ , 5 mM azide and the GLUT blocker cytochalasin B (20  $\mu$ M). After transiently withdrawing glucose for calibration purposes, cultures were superfused with a buffer devoid of BHB, followed by reapplication of  $K^+$ , azide and cytochalasin. Bars represent the average extent of glucose depletion measured at the end of the stimulations in three separate experiments (20–30 cells per experiment). Previous experiments showed that glucose metabolism in astrocytes is not affected by transient glucose depletion.<sup>21</sup>

(Figure 2a). The strong stimulation of astrocytic glycolysis that is normally observed in response to inhibition of oxidative phosphorylation (OXPHOS) was also blunted by BHB treatment (Figure 2b), despite significant ATP depletion, as detected independently with the FRET ATP nanosensor ATeam<sup>18</sup> and the fluorescent probe Magnesium Green (Figures 2c–f). The effects of the ketone body were reversible. In the experiment illustrated in Figure 3 astrocytes that had been treated with BHB for 3 days displayed a small response to high  $K^+$  and negligible rates of glucose consumption and response to OXPHOS inhibition. Removal of BHB led to a significant recovery of all three parameters, indicating that the metabolic modulation requires the continued presence of BHB and that it involves signals acting in the order of minutes.

Ketone bodies are oxidized in mitochondria. To test for possible effects of BHB on mitochondrial metabolism, we measured the capacity of astrocytic mitochondria to metabolize pyruvate using the genetically-encoded FRET nanosensor Pyronic according to a protocol described previously.<sup>19</sup> In brief, cells expressing the sensor (Figure 4a) were first incubated in a buffer containing pyruvate as sole energy substrate, and then exposed to a cocktail of inhibitors of pyruvate transport at the plasma membrane. We have observed that in astrocytes in culture the uptake of pyruvate is partly mediated by an AR-C155858-sensitive MCT<sup>36</sup> and partly by a pathway sensitive to the non-specific inhibitor probenecid (Garrido-Gerter, P. and Barros, L.F., unpublished data). The rate of decrease in the concentration of pyruvate after inhibition of both

pathways is therefore equivalent to the rate of pyruvate consumption by mitochondria (Figure 4b and literature<sup>19</sup>). As shown in Figure 4(c), a 3-day exposure of astrocytes to BHB caused a small but significant increase in mitochondrial pyruvate consumption. This enhancement of the ability of BHB-treated astrocytes to metabolize pyruvate suggests that the reduction of glycolysis is not explained by a decrease in pyruvate uptake by mitochondria but by an inhibition of glycolysis, possibly by enhanced mitochondrial ATP production from BHB. The steady-state cytosolic concentration of pyruvate in pyruvate-bathed cells was higher in BHB-treated cells than in control cells ( $103 \pm 3 \mu$ M and  $81 \pm 2 \mu$ M, respectively,  $n = 6$  experiments) despite their higher consumption, pointing to parallel upregulation of pyruvate transport at the cell surface. Confirming this notion, BHB treatment significantly increased MCT activity (Figure 4d and e), computed as the rate of intracellular acidification in response to either lactate or BHB.<sup>37</sup> This increase in MCT activity may be interpreted as an adaptive response to the presence of BHB.

Next, the glucose sensor was expressed in protoplasmic astrocytes in organotypic hippocampal slices (Figure 5a), prepared according to a revised protocol that optimizes the functional and metabolic properties of the tissue.<sup>38</sup> As with cultured cells, a 3-day treatment of tissue slices with BHB provoked a marked inhibition of astrocytic glucose consumption (Figure 5b). To approach the effect of ketone bodies in vivo, the rate of astrocytic glucose consumption was measured by FRET in acute hippocampal slices prepared from

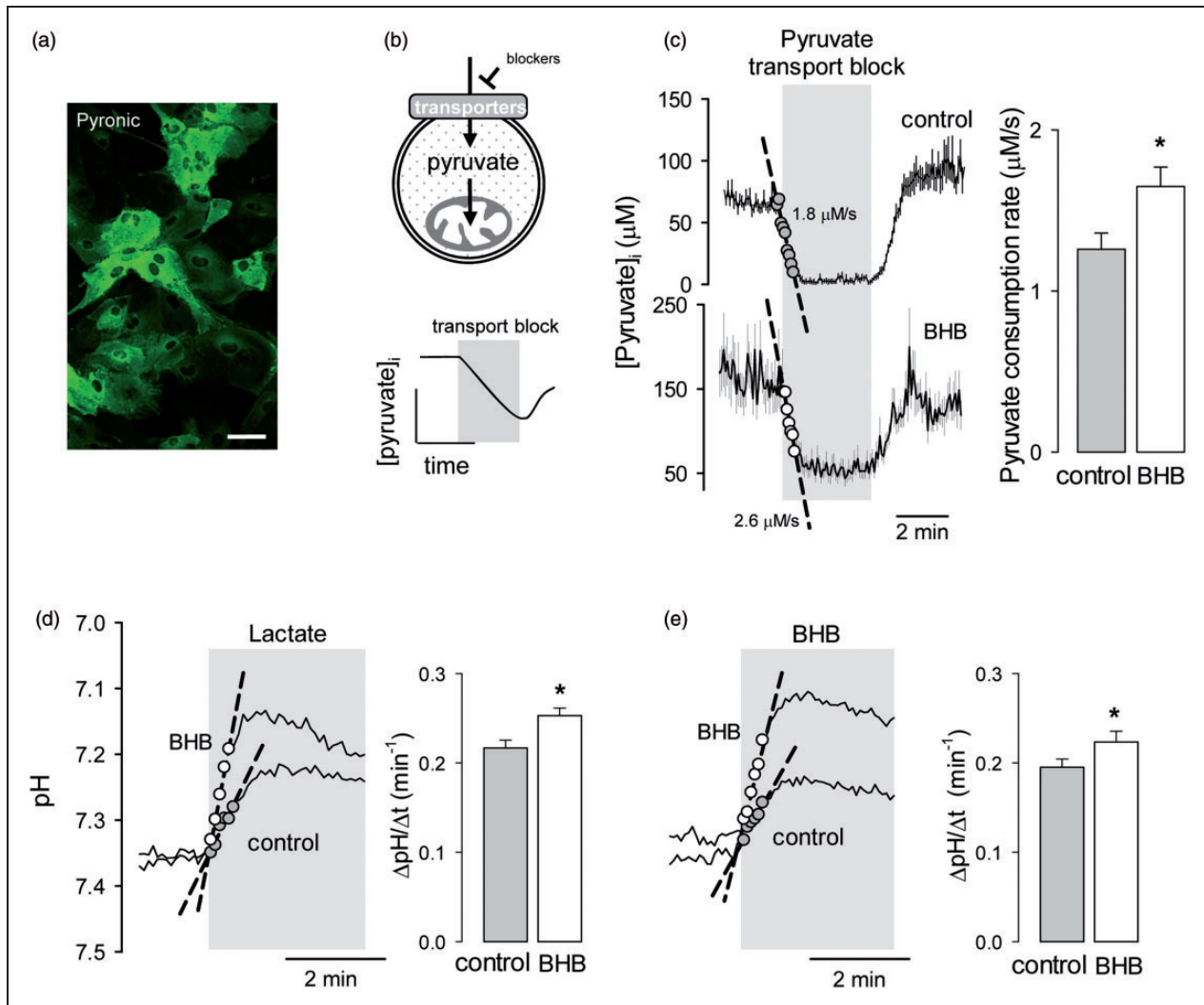


**Figure 4.** Chronic BHB exposure stimulates mitochondrial pyruvate consumption and surface MCT activity. (a) Expression of the pyruvate sensor Pyronic in astrocytes of mixed cortical cultures. Bar = 50  $\mu\text{m}$ . (b) Rationale of the method to measure the rate of mitochondrial pyruvate consumption by monitoring cytosolic pyruvate in the presence of the pyruvate transport blockers AR-C155858 (1  $\mu\text{M}$ ) and probenecid (1 mM). (c) Measurement of pyruvate consumption rates of astrocytes exposed for 3 days to control conditions (gray symbols) or to 2 mM BHB (open symbols). Bars represent the average rates obtained in three separate experiments (20–30 cells per experiment). Monocarboxylate transporter activity was measured by monitoring the rate of intracellular acidification in the presence of 10 mM lactate (d) or 10 mM BHB (e) in control cells or in cell treated for 3 days with 2 mM BHB. Bars represent the average rates obtained in six separate experiments (10–20 cells per experiment).

ketotic animals (Figure 6a). Firstly, a recombinant adeno-associated virus coding for FLII12Pglu700 $\mu\Delta$ 6 under the control of the short gfaABC1D promoter was stereotactically injected into the hippocampus of 3-month-old mice. After an expression time of 6 weeks, the animals were food-deprived for 36 h to induce ketosis,<sup>39</sup> which was confirmed by a marked increase in ketone body urine concentration (Figure 6b). At the end of the starvation period, the animals were euthanized and hippocampal slices were prepared,<sup>22</sup> followed by estimation of glucose consumption by FRET

microscopy. To prevent loss of ketone body effect (Figure 3), the brain slices of food-deprived animals were prepared in the presence of 2 mM BHB. Food-deprivation had no apparent effect on the general level of activity of the animals. Imaged in acute hippocampal slices, protoplasmic astrocytes showed their typical size and morphology, with small somata and abundant branching processes (Figure 6c). Application of the GLUT block protocol showed a significant decrease in the rate of astrocytic glucose consumption in slices prepared from ketotic animals (Figure 6c).

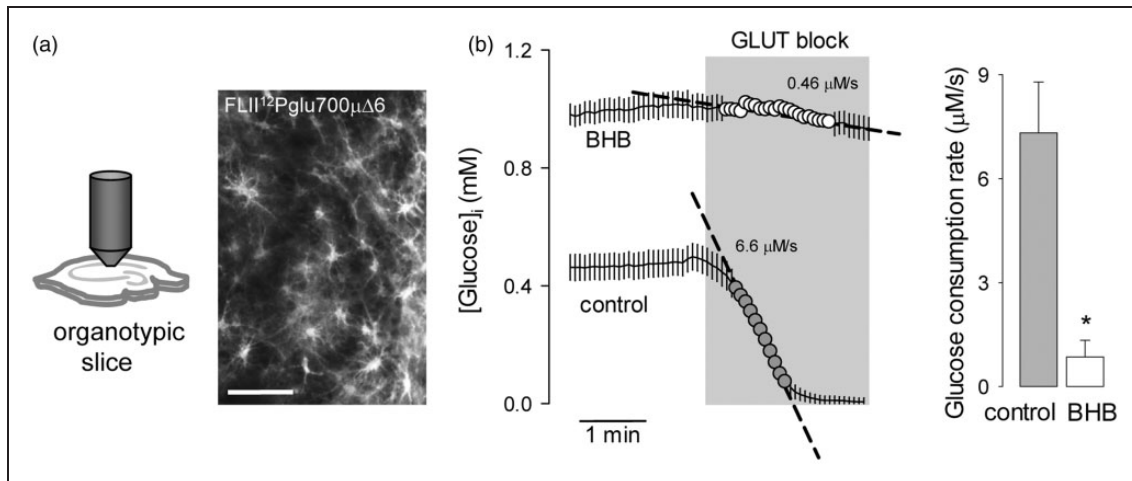


**Figure 5.** Chronic BHB exposure inhibits astrocytic glycolysis in organotypic hippocampal slices. (a) Expression of the glucose sensor FLII<sup>12</sup>Pglu700 $\mu\Delta$ 6 in astrocytes in organotypic hippocampal slices. Bar = 100  $\mu$ m. (b) Measurement of astrocytic glucose consumption rate with 20  $\mu$ M cytochalasin B in organotypic slices exposed for 3 days to control conditions (gray symbols) or to 2 mM BHB (open symbols). Bars represent the average rates obtained in three separate experiments (8–10 cells per experiment).

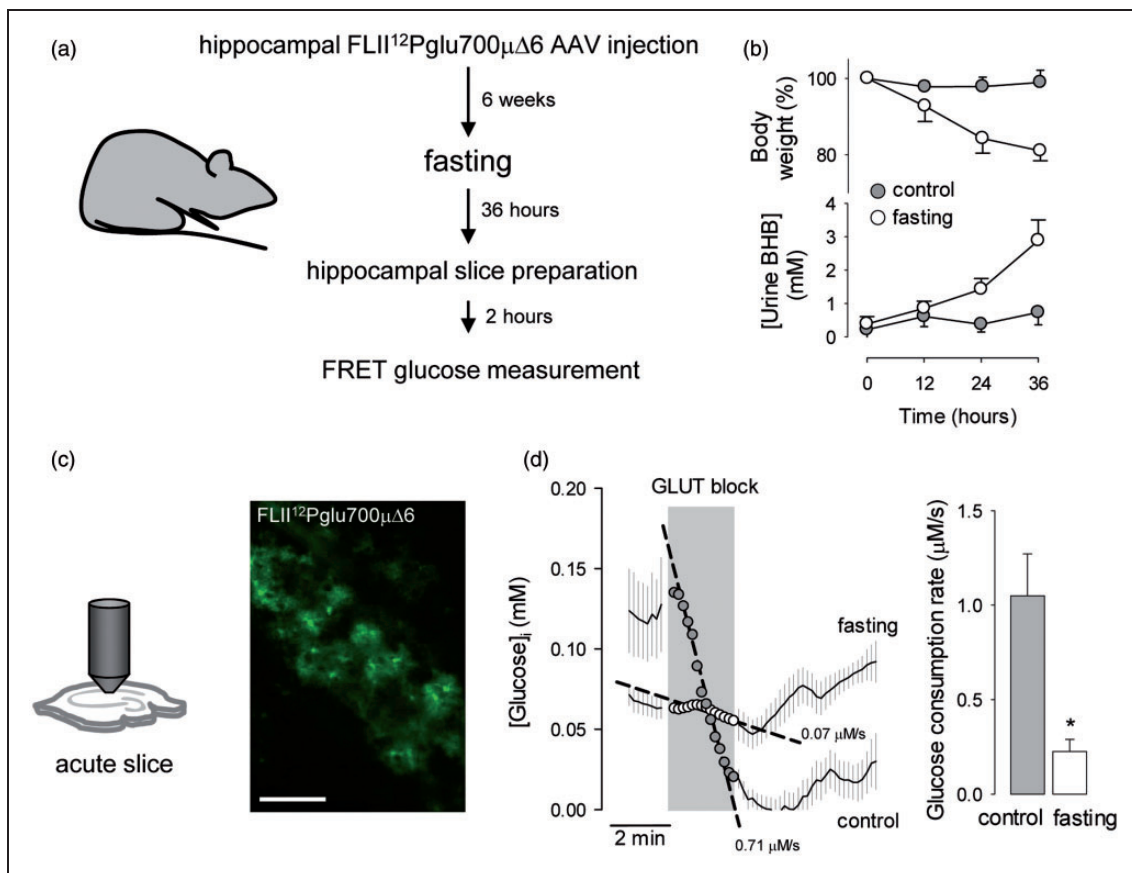


**Figure 6.** Inhibition of astrocytic glycolysis in ketotic mice. (a) Protocol for the estimation of astrocytic glucose consumption in ketotic mice. (b) Effect of food deprivation on body weight and ketone body concentration in urine. (c) Expression of the glucose sensor FLII<sup>12</sup>Pglu700 $\mu\Delta$ 6 in astrocytes in acute hippocampal slices. Bar = 100  $\mu$ m. (d) Measurement of astrocytic glucose consumption rate with 20  $\mu$ M cytochalasin B in acute hippocampal slices of control (gray symbols) and 36-h fasting mice (open symbols). Bars represent the average rates obtained in three separate experiments (5–8 cells per experiment).

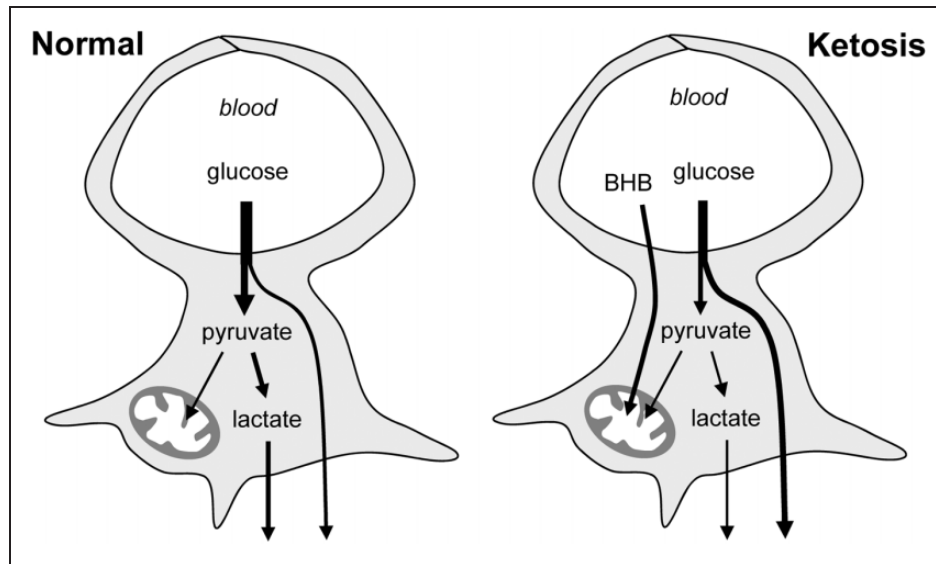


**Figure 7.** Modification of astrocytic glucose dynamics by BHB. Under normal conditions glucose enters astrocytes where a fraction is metabolized to lactate. During ketosis, BHB is efficiently metabolized by mitochondria and astrocytic glycolysis becomes inhibited. This increases the availability of glucose to neurons and reduces their exposure to lactate.

## Discussion

We report a strong inhibitory effect of chronic exposure to the ketone body BHB on the consumption of glucose by astrocytes and on the capacity of astrocytic glycolysis to respond to physiological and pathological stimuli. However, the ability of astrocytes to metabolize pyruvate was unaffected by BHB. These findings suggest that the reduction of whole brain glucose consumption observed during ketosis involves astrocytes. Considering the importance of astrocytic glucose and lactate for neuronal function and survival, we propose that the modulation of astrocytic glucose metabolism by ketone bodies contributes to neuroprotection.

The reduction of astrocytic glucose consumption in response to BHB was a robust phenomenon, observed in cultured cells and in protoplasmic astrocytes in organotypic hippocampal slices. Lower astrocytic glucose consumption was also found in acute hippocampal slices prepared from animals that had been made ketotic by food deprivation. Furthermore, BHB severely impaired the ability of astrocytes to upregulate their glycolysis in response to  $K^+$ , a mechanism whereby active neurons acutely stimulate astrocytic glycolysis and lactate release.<sup>32–34</sup> BHB also blunted the response of astrocytic glycolysis to chemical anoxia, despite ATP depletion of similar extent to that observed in control cells. This suppression of the Pasteur Effect suggests that ketone bodies interfere with the regulatory interaction between mitochondria and the glycolytic machinery. As astrocytes consume glucose and are interposed between neurons and the vasculature,<sup>11</sup> a weaker glycolysis in the presence of BHB

is predicted to increase the availability of glucose for neuronal usage (Figure 7). A reduced glycolysis may also impair astrocytic lactate export, a process thought to be involved in intercellular signaling and fueling, whose extent is a matter of current debate and investigation. Underscoring the role of glucose metabolism in epilepsy, pharmacological inhibition of lactate dehydrogenase (LDH) decreased neuronal excitability and protected against seizures.<sup>40</sup>

Multiple mechanisms contribute to the neuroprotective effect of ketone bodies. Neurons can effectively utilize ketone bodies,<sup>7,10,41,42</sup> leading to the activation of the neuronal potassium channel  $K_{ATP}$ .<sup>43</sup> Consistently, reduced glucose oxidation in Bcl-2-associated death (BAD) knockout mice conferred resistance to seizures, an effect shown to be mediated by  $K_{ATP}$  channels.<sup>8</sup> In addition, ketone bodies have been shown to compete with the chloride binding site at synaptic glutamate vesicles, thereby reducing excitatory neurotransmission.<sup>44</sup> The importance of appropriate glucose delivery to neurons is highlighted by the observation that GLUT1 reductions in the blood-brain barrier – but not in astrocytes – exacerbate neurological abnormalities in a mouse model of Alzheimer's disease.<sup>5</sup> In this context, astrocytic glycolysis and astrocytic lactate release and the mechanisms that modulate them in response to neuronal activity may be considered therapeutic targets.

## Funding

The author(s) disclosed receipt of the following financial support for the research, authorship, and/or publication of this article: This research was partly supported by a joint grant



from the Comisión Nacional de Investigación Científica y Tecnológica (CONICYT)-Chile and the Deutsche Forschungsgemeinschaft (DFG) to LFB and JWD (DFG-12, DE 231/25-1) and by Fondecyt 1130095 to LFB. The Centro de Estudios Científicos (CECs) is funded by the Chilean Government through the Centers of Excellence Basal Financing Program of CONICYT.

### Acknowledgements

We thank Karen Everett for critical reading of the manuscript and Dr Bruno Weber for kindly providing the FLIII2Pglu700 $\mu$  $\Delta$ 6 AAV vector.

### Declaration of conflicting interests

The author(s) declared no potential conflicts of interest with respect to the research, authorship, and/or publication of this article.

### Authors' contributions

Designed research: IR, HMB, JDW, LFB; Performed research: RV, IR, PG, IF, LF, KA; Analyzed data: RV, IR, PG, IF, LF, HMB, JWD; Wrote the paper: LFB.

### References

- Pascual JM, Wang D, Lecumberri B, et al. GLUT1 deficiency and other glucose transporter diseases. *Eur J Endocrinol* 2004; 150: 627–633.
- Klepper J, Wang D, Fischbarg J, et al. Defective glucose transport across brain tissue barriers: a newly recognized neurological syndrome. *Neurochem Res* 1999; 24: 587–594.
- Klepper J and Leidencker B. Glut1 deficiency syndrome and novel ketogenic diets. *J Child Neurol* 2013; 28: 1045–1048.
- Maalouf M, Rho JM and Mattson MP. The neuroprotective properties of calorie restriction, the ketogenic diet, and ketone bodies. *Brain Res Rev* 2009; 59: 293–315.
- Winkler EA, Nishida Y, Sagare AP, et al. GLUT1 reductions exacerbate Alzheimer's disease vasculo-neuronal dysfunction and degeneration. *Nat Neurosci* 2015; 18: 521–530.
- Zhang Y, Kuang Y, Xu K, et al. Ketosis proportionately spares glucose utilization in brain. *J Cereb Blood Flow Metab* 2013; 33: 1307–1311.
- Chowdhury GM, Jiang L, Rothman DL, et al. The contribution of ketone bodies to basal and activity-dependent neuronal oxidation in vivo. *J Cereb Blood Flow Metab* 2014; 34: 1233–1242.
- Gimenez-Cassina A, Martinez-Francois JR, Fisher JK, et al. BAD-dependent regulation of fuel metabolism and K(ATP) channel activity confers resistance to epileptic seizures. *Neuron* 2012; 74: 719–730.
- Lutas A and Yellen G. The ketogenic diet: metabolic influences on brain excitability and epilepsy. *Trends Neurosci* 2013; 36: 32–40.
- Edmond J, Robbins RA, Bergstrom JD, et al. Capacity for substrate utilization in oxidative metabolism by neurons, astrocytes, and oligodendrocytes from developing brain in primary culture. *J Neurosci Res* 1987; 18: 551–561.
- Mathiisen TM, Lehre KP, Danbolt NC, et al. The perivascular astroglial sheath provides a complete covering of the brain microvessels: an electron microscopic 3D reconstruction. *Glia* 2010; 58: 1094–1103.
- Schurr A, West CA and Rigor BM. Lactate-supported synaptic function in the rat hippocampal slice preparation. *Science* 1988; 240: 1326–1328.
- Wyss MT, Jolivet R, Buck A, et al. In vivo evidence for lactate as a neuronal energy source. *J Neurosci* 2011; 31: 7477–7485.
- Herrero-Mendez A, Almeida A, Fernandez E, et al. The bioenergetic and antioxidant status of neurons is controlled by continuous degradation of a key glycolytic enzyme by APC/C-Cdh1. *Nat Cell Biol* 2009; 11: 747–752.
- Bak LK, Schousboe A, Sonnewald U, et al. Glucose is necessary to maintain neurotransmitter homeostasis during synaptic activity in cultured glutamatergic neurons. *J Cereb Blood Flow Metab* 2006; 26: 1285–1297.
- Fernandez-Fernandez S, Almeida A and Bolanos JP. Antioxidant and bioenergetic coupling between neurons and astrocytes. *Biochem J* 2012; 443: 3–11.
- Takanaga H, Chaudhuri B and Frommer WB. GLUT1 and GLUT9 as major contributors to glucose influx in HepG2 cells identified by a high sensitivity intramolecular FRET glucose sensor. *Biochim Biophys Acta* 2008; 1778: 1091–1099.
- Imamura H, Nhat KP, Togawa H, et al. Visualization of ATP levels inside single living cells with fluorescence resonance energy transfer-based genetically encoded indicators. *Proc Natl Acad Sci U S A* 2009; 106: 15651–15656.
- San Martín A, Ceballo S, Baeza-Lehnert F, et al. Imaging mitochondrial flux in single cells with a FRET sensor for pyruvate. *PLoS ONE* 2014; 9: e85780.
- Dirren E, Towne CL, Setola V, et al. Intracerebroventricular injection of adeno-associated virus 6 and 9 vectors for cell type-specific transgene expression in the spinal cord. *Hum Gene Ther* 2014; 25: 109–120.
- Bittner CX, Loaiza A, Ruminot I, et al. High resolution measurement of the glycolytic rate. *Front Neuroenergetics* 2010; 2: 1–11.
- Jakoby P, Schmidt E, Ruminot I, et al. Higher transport and metabolism of glucose in astrocytes compared with neurons: a multiphoton study of hippocampal and cerebellar tissue slices. *Cereb Cortex* 2014; 24: 222–231.
- Schneider J, Lewen A, Ta TT, et al. A reliable model for gamma oscillations in hippocampal tissue. *J Neurosci Res* 2015; 93: 1067–1078.
- Hou BH, Takanaga H, Grossmann G, et al. Optical sensors for monitoring dynamic changes of intracellular metabolite levels in mammalian cells. *Nat Protoc* 2011; 6: 1818–1833.
- Barros LF, Baeza-Lehnert F, Valdebenito R, et al. Fluorescent nanosensor based flux analysis: overview and the example of glucose. In: Waagepetersen HS and Hirrlinger J (eds) *Springer protocols: Brain energy metabolism*. Berlin: Springer, 2014.

26. San Martín A, Sotelo-Hitschfeld T, Lerchundi R, et al. Single-cell imaging tools for brain energy metabolism: a review. *Neurophotonics* 2014; 1.
27. Walz W. Swelling and potassium uptake in cultured astrocytes. *Can J Physiol Pharmacol* 1987; 65: 1051–1057.
28. Gjedde A and Diemer NH. Autoradiographic determination of regional brain glucose content. *J Cereb Blood Flow Metab* 1983; 3: 303–310.
29. Alf MF, Wyss MT, Buck A, et al. Quantification of brain glucose metabolism by 18F-FDG PET with real-time arterial and image-derived input function in mice. *J Nucl Med* 2013; 54: 132–138.
30. Kaminski MT, Lenzen S and Baltrusch S. Real-time analysis of intracellular glucose and calcium in pancreatic beta cells by fluorescence microscopy. *Biochim Biophys Acta* 2012; 1823: 1697–1707.
31. Deves R and Krupka RM. Cytochalasin B and the kinetics of inhibition of biological transport: a case of asymmetric binding to the glucose carrier. *Biochim Biophys Acta* 1978; 510: 339–348.
32. Bittner CX, Valdebenito R, Ruminot I, et al. Fast and reversible stimulation of astrocytic glycolysis by  $K^+$  and a delayed and persistent effect of glutamate. *J Neurosci* 2011; 31: 4709–4713.
33. Ruminot I, Gutiérrez R, Peña-Munzenmeyer G, et al. NBCe1 mediates the acute stimulation of astrocytic glycolysis by extracellular  $K^+$ . *J Neurosci* 2011; 31: 14264–14271.
34. Sotelo-Hitschfeld T, Niemeyer MI, Machler P, et al. Channel-mediated lactate release by  $K^+$ -stimulated astrocytes. *J Neurosci* 2015; 35: 4168–4178.
35. Frohlich F, Bazhenov M, Iragui-Madoz V, et al. Potassium dynamics in the epileptic cortex: new insights on an old topic. *Neuroscientist* 2008; 14: 422–433.
36. Ovens MJ, Davies AJ, Wilson MC, et al. AR-C155858 is a potent inhibitor of monocarboxylate transporters MCT1 and MCT2 that binds to an intracellular site involving transmembrane helices 7–10. *Biochem J* 2010; 425: 523–530.
37. Broer S, Schneider HP, Broer A, et al. Characterization of the monocarboxylate transporter 1 expressed in *Xenopus laevis* oocytes by changes in cytosolic pH. *Biochem J* 1998; 333: 167–174.
38. Galow LV, Schneider J, Lewen A, et al. Energy substrates that fuel fast neuronal network oscillations. *Front Neurosci* 2014; 8: 398.
39. Jiang L, Mason GF, Rothman DL, et al. Cortical substrate oxidation during hyperketonemia in the fasted anesthetized rat in vivo. *J Cereb Blood Flow Metab* 2011; 31: 2313–2323.
40. Sada N, Lee S, Katsu T, et al. Epilepsy treatment. Targeting LDH enzymes with a stiripentol analog to treat epilepsy. *Science* 2015; 347: 1362–1367.
41. Lopes-Cardozo M, Larsson OM and Schousboe A. Acetoacetate and glucose as lipid precursors and energy substrates in primary cultures of astrocytes and neurons from mouse cerebral cortex. *J Neurochem* 1986; 46: 773–778.
42. McKenna MC, Tildon JT, Stevenson JH, et al. Lactate transport by cortical synaptosomes from adult rat brain: characterization of kinetics and inhibitor specificity. *Dev Neurosci* 1998; 20: 300–309.
43. Ma W, Berg J and Yellen G. Ketogenic diet metabolites reduce firing in central neurons by opening  $K(ATP)$  channels. *J Neurosci* 2007; 27: 3618–3625.
44. Juge N, Gray JA, Omote H, et al. Metabolic control of vesicular glutamate transport and release. *Neuron* 2010; 68: 99–112.